The Canadian Mineralogist
Vol. 45, pp. 321-333 (2007)

COMPLEX TWINNING, POLYTYPISM AND DISORDER PHENOMENA IN THE CRYSTAL STRUCTURES OF ANTIMONPEARCEITE AND ARSENPOLYBASITE

LUCA BINDI[§]

Museo di Storia Naturale, Sezione di Mineralogia, Università degli Studi di Firenze, via La Pira 4, I–50121 Firenze, Italy

MICHEL EVAIN

Laboratoire de Chimie des Solides, I.M.N., UMR C6502 CNRS – Université de Nantes, 2, rue de la Houssinière, BP 32229, F–44322 Nantes Cedex 3, France

SILVIO MENCHETTI

Dipartimento di Scienze della Terra, Università degli Studi di Firenze, via La Pira 4, I–50121 Firenze, Italy

ABSTRACT

The crystal structures of antimonpearceite, arsenpolybasite-222 and arsenpolybasite-221 have been solved and refined from single-crystal X-ray-diffraction datasets. Antimonpearceite crystallizes in the trigonal space-group $P\bar{3}m1$, with a 7.4805(5), c 11.8836(13) Å, V 575.89(8) Å^3 and Z = 1. The refinement of the structure leads to R = 0.0352 for 1095 independent observed reflections [$I/\sigma(I) \geq 2$] and 98 parameters. Arsenpolybasite-222 crystallizes in the monoclinic space-group $C2/c$, with a 26.036(2), b 15.0319(13), c 24.042(3) Å, β 90.000(13)° (pseudohexagonal cell with the $a = \sqrt{3}b$ orthohexagonal relation), V 9409.5(15) Å^3 and Z = 16. A second-degree twinning by metric merohedry gives rise to an apparent trigonal symmetry, with the unit-cell parameters (hexagonal cell) a 15.0319(13) and c 24.042(3) Å. The refinement of the structure leads to R = 0.0716 for 22008 independent observed reflections [$I/\sigma(I) \geq 2$] and 552 parameters. Arsenpolybasite-221 crystallizes in the space group $P321$, with a 14.9746(17), c 11.9982(6) Å, V 2330.0(4) Å^3 and Z = 4. The refinement of the structure, including a mirror-twin operation (first-degree twin, $\bar{3}'2/m'1$ polychromatic point-group), leads to R = 0.0434 for 4639 independent observed reflections [$I/\sigma(I) \geq 2$] and 184 parameters. All the structures consist of the stacking of $[(Ag,Cu)_6(As,Sb)_2S_7]^{2-}$ and $[Ag_9CuS_4]^{2+}$ module layers along [001]; (As,Sb) forms isolated $(As,Sb)S_3$ pyramids typically occurring in sulfosalts, copper links two sulfur atoms in a linear coordination, and silver occupies sites with coordination ranging from quasilinear to almost tetrahedral. The substitution of Cu for Ag in the $[(Ag,Cu)_6(As,Sb)_2S_7]^{2-}$ module layer becomes greater in going from the 111 structure, through the 221, to the 222 structure. The determination of the crystal structure for all the members of the group leads us to consider them as a family of polytypes.

Keywords: antimonpearceite, arsenpolybasite, polytypism, disorder, twinning, crystal-structure determination.

SOMMAIRE

Nous avons résolu et affiné la structure cristalline de l'antimonpearceïte, l'arsenpolybasite-222 et l'arsenpolybasite-221 à partir de données en diffraction X prélevées sur monocristaux. L'antimonpearceïte cristallise dans le groupe spatial $P\bar{3}m1$, système trigonal, avec a 7.4805(5), c 11.8836(13) Å, V 575.89(8) Å^3 et Z = 1. L'affinement de la structure a mené à un R égal à 0.0352 pour 1095 réflexions indépendantes observées [$I/\sigma(I) \geq 2$] et 98 paramètres. L'arsenpolybasite-222 cristallise dans le groupe spatial $C2/c$, système monoclinique, avec a 26.036(2), b 15.0319(13), c 24.042(3) Å, β 90.000(13)° (maille pseudohexagonale avec la relation orthohexagonale ayant la relation $a = \sqrt{3}b$), V 9409.5(15) Å^3 et Z = 16. Une macle de second degré par méroédrie métrique produit une symétrie trigonale apparente, avec les paramètres réticulaires (maille hexagonale) a 15.0319(13) et c 24.042(3) Å. L'affinement de la structure a mené à un R égal à 0.0716 pour 22008 réflexions indépendantes observées [$I/\sigma(I) \geq 2$] et 552 paramètres. L'arsenpolybasite-221 cristallise dans le groupe spatial $P321$, avec a 14.9746(17), c 11.9982(6) Å, V 2330.0(4) Å^3 et Z = 4. L'affinement de la structure, qui comprend une opération de macle mirroir (macle de premier degré, groupe ponctuel polychromatique $\bar{3}'2/m'1$), a mené à un R égal à 0.0434 pour 4639 réflexions indépendantes observées [$I/\sigma(I) \geq 2$] et 184 paramètres. Ces trois structures sont faites d'un empilement de modules $[(Ag,Cu)_6(As,Sb)_2S_7]^{2-}$ et $[Ag_9CuS_4]^{2+}$ en couches le long de [001]; le (As,Sb) forme des pyramides $(As,Sb)S_3$ isolées typiques des sulfosels, avec le cuivre lié à deux atomes de soufre en coordinence linéaire, et les atomes d'argent en coordinence quasiment linéaire à tétraédrique. Avec une substitution du Cu pour Ag, le volume du module en couche $[(Ag,Cu)_6(As,Sb)_2S_7]^{2-}$ augmente de la structure 111 à la structure 221, et enfin à la structure 222. La détermination de la structure des trois membres du groupe nous pousse à les considérer une famille de polytypes.

Mots-clés: antimonpearceïte, arsenpolybasite, polytypisme, désordre, macles, détermination de la structure.

§ *E-mail address*: lbindi@geo.unifi.it

Introduction

The minerals belonging to the pearceite–polybasite group were divided by Frondel (1963) into two series: the first one, involving pearceite $[(Ag,Cu)_{16}(As,Sb)_2S_{11}]$ and antimonpearceite $[(Ag,Cu)_{16}(Sb,As)_2S_{11}]$, is characterized by a "small" unit-cell [labeled 111] and a high Cu content; the second one, with polybasite $[(Ag,Cu)_{16}(Sb,As)_2S_{11}]$ and arsenpolybasite $[(Ag,Cu)_{16}(As,Sb)_2S_{11}]$, has doubled unit-cell parameters [labeled 222] and a low Cu content. Moreover, the existence of an intermediate type of unit cell, labeled 221, was claimed for both polybasite (Harris *et al.* 1965, Edenharter *et al.* 1971) and arsenpolybasite (Minčeva-Stefanova *et al.* 1979). From the crystallographic point of view, these minerals were initially reported as being monoclinic *C*2/*m*, although dimensionally pseudo-hexagonal (Peacock & Berry 1947, Frondel 1963, Harris *et al.* 1965, Hall 1967, Sugaki *et al.* 1983). Recently, Bindi *et al.* (2006a) solved and refined the crystal structure of pearceite in the space group $P\bar{3}m1$. They showed that the structure of pearceite can be described as a regular alternation of two kinds of layer stacked along the **c** axis: a first layer (labeled A), of general composition $[(Ag,Cu)_6(As,Sb)_2S_7]^{2-}$, and a second layer (labeled B), with a general composition $[Ag_9CuS_4]^{2+}$. The complex polytypism phenomena (*i.e.,* 221 and 222 unit-cell types) occurring in various samples of polybasite were studied by Evain *et al.* (2006a). These authors solved and refined the crystal structure of both polybasite-221 (space group *P*321) and polybasite-222 (space group *C*2/*c*), and proposed a possible mechanism regulating the stabilization of unit-cell type in these minerals. Finally, by means of a study of a crystal of Se-rich antimonpearceite (with 2.55 atoms per formula unit Se), Evain *et al.* (2006b) investigated the structural role of selenium in these minerals.

In this paper, we report the structural characterization of the remaining members of the pearceite–polybasite group, antimonpearceite, arsenpolybasite-222 and arsenpolybasite-221.

Background Information

A summary of all known cell metrics and space groups in the pearceite–polybasite group is given in Table 1. To describe the complex electron-density associated with Ag,Cu observed in these structures, Bindi *et al.* (2006a) and Evain *et al.* (2006a, b) used a non-harmonic model based upon a development of the atomic displacement factor (Kuhs & Heger 1979, Boucher *et al.* 1993, Evain *et al.* 1998). In general, in the presence of atomic disorder, a split-atom approach is classically used in structure determinations. However, that approach has several disadvantages, and gives rise to ambiguities. As Bachmann & Schulz (1984) have demonstrated, the introduction of extra positions in the refinement does not necessarily means that those positions correspond to occupied equilibrium sites. This is particularly true in the case of fast ionic conductors, for which there exists a delocalization of an ionic species over a liquid-like structure, and also where cations such as a d^{10} element easily adopt a complicated coordination because of *s*,*d* orbital mixing or polarization factors (Gaudin *et al.* 2001). In addition to the problem of the physical meaning of the refined positions, one usually observes that the closer the refined positions in a disordered structure, the higher the correlations and the more unstable the refinements. The use of tensor elements of higher order in the expression of the structure factors (the "non-harmonic approach") is then an alternative solution, giving an equivalent description (Kuhs 1992). The benefit of the latter description over the split-atom model is an easier convergence of the refinement as a result of much lower correlations among the refined parameters, as proven in many structure determinations (see for instance the case of argyrodite: Boucher *et al.* 1993). In both cases, however, the refined coordinates do not have a simple physical meaning, because they are simply the first-order terms in the expansion of the conventional structure-factor. Therefore, one must be very cautious in interpreting bond distances from such refinements. A better way to interpret the refined parameters is by using the joint probability-density function

TABLE 1. CELL METRICS, CELL TRANSFORMATIONS AND SPACE GROUPS IN THE PEARCEITE – POLYBASITE SYSTEM

cell metrics	cell transformation	space group	mineral	reference
$a \times a \times c$	**a**, **b**, **c**	$P\bar{3}m1$	pearceite	Bindi *et al.* (2006a)
$a \times a \times c$	**a**, **b**, **c**	$P\bar{3}m1$	antimonpearceite	this study
$2a \times 2a \times c$	2**a**, 2**b**, **c**	*P*321	polybasite-221	Evain *et al.* (2006a)
$2a \times 2a \times c$	2**a**, 2**b**, **c**	*P*321	arsenpolybasite-221	this study
$2a\sqrt{3} \times 2a \times 2c$, $\beta \approx 90°$	4**a** + 2**b**, 2**b**, 2**c**	*C*2/*c*	polybasite-222	Evain *et al.* (2006a)
$2a\sqrt{3} \times 2a \times 2c$, $\beta = 90°$	4**a** + 2**b**, 2**b**, 2**c**	*C*2/*c*	arsenpolybasite-222	this study
$a\sqrt{3} \times a \times 2c$, $\beta = 90°$	2**a** + **b**, **b**, 2**c**	$P2_1/c$	Se-rich antimonpearceite	Evain *et al.* (2006b)

(*jpdf*), which can be directly calculated from the refined parameters. This function is the weighted superposition of the Fourier transform of the non-harmonic atom-displacement factors of atoms over several sites.

Occurrence and Chemical Composition

The samples investigated, antimonpearceite (catalog number 171541, Smithsonian Institution, Washington), arsenpolybasite-222 (catalog number AW634, Naturhistorisches Museum of Vienna) and arsenpolybasite-221 (catalog number AB6829, Naturhistorisches Museum of Vienna), are from different localities: the Eagle mine, Colorado, St. Joachimsthal (Bohemia), and Freiberg (Germany), respectively.

A preliminary chemical analysis using energy-dispersive spectrometry, performed on the crystal fragments used for the structural study, did not indicate the presence of elements ($Z > 9$) other than S, Fe, Cu, Zn, As, Se, Ag, Sb, Te, Au, Pb, and Bi. The chemical composition was then determined using wavelength-dispersive analysis (WDS) by means of a JEOL JXA–8200 electron microprobe. Concentrations of major and minor elements were determined at a 20 kV accelerating voltage and a 40 nA beam current, with 10 s as counting time. For the WDS analyses, the following lines were used: S$K\alpha$, Fe$K\alpha$, Cu$K\alpha$, Zn$K\alpha$, As$L\alpha$, Se$L\alpha$, Ag$L\alpha$, Sb$L\beta$, Te$L\alpha$, Au$M\alpha$, Pb$M\alpha$, and Bi$M\beta$. The estimated analytical precision (wt%) is: ±0.55 for Ag, ±0.40 for Sb, ±0.30 for Cu, ±0.20 for S, ±0.05 for As and Se, ±0.01 for Fe, Zn, Te, Au, Pb and Bi. The standards employed were: native elements for Cu, Ag, Au, and Te, galena for Pb, pyrite for Fe and S, synthetic Sb_2S_3 for Sb, synthetic As_2S_3 for As, synthetic Bi_2S_3 for Bi, synthetic ZnS for Zn, and synthetic $PtSe_2$ for Se. The crystal fragments were found to be homogeneous within analytical error. The average chemical compositions (four to six analyses on each grain), together with ranges of wt% of elements, are reported in Table 2. On the basis of 29 atoms, the formulae can be written as $(Ag_{13.10}Cu_{2.91}Zn_{0.01}Fe_{0.01})_{\Sigma 16.03}(Sb_{1.73}As_{0.17})_{\Sigma 1.90}(S_{11.07}Te_{0.01})_{\Sigma 11.08}$, $(Ag_{14.77}Cu_{1.08}Bi_{0.01}Pb_{0.01}Fe_{0.01}Au_{0.01})_{\Sigma 15.89}(As_{1.75}Sb_{0.08})_{\Sigma 1.83}(S_{11.23}Te_{0.03})_{\Sigma 11.26}$ and $(Ag_{14.64}Cu_{1.55}Zn_{0.01}Bi_{0.02}Au_{0.01})_{\Sigma 16.23}(As_{1.76}Sb_{0.01})_{\Sigma 1.77}(S_{10.95}Se_{0.01}Te_{0.01})_{\Sigma 10.97}$ for the antimonpearceite, arsenpolybasite-222 and arsenpolybasite-221 crystals, respectively. It is worth noting that the sum (Sb + As) is considerably less than 2 in the chemical formulae; this feature could be related to the sensitivity shown by these minerals to the electron beam.

X-Ray Crystallography and Crystal-Structure Determination

All the data collections were carried out on a Bruker–Nonius Kappa CCD diffractometer using graphite-monochromatized MoK–$L_{2,3}$ radiation. In expectation of possible twinning, special care was taken with the choice of the fraction of reciprocal space covered. Intensity integration and standard

TABLE 2. COMPOSITIONS (ELECTRON-MICROPROBE DATA) AND ATOM RATIOS GIVEN WITH THEIR STANDARD DEVIATIONS (σ) FOR THE CRYSTALS SELECTED

	antimonpearceite 171541				arsenpolybasite–221 AB6829				arsenpolybasite–222 AW634			
	mean	range	ratio	(σ)	mean	range	ratio	(σ)	mean	range	ratio	(σ)
Ag wt.%	64.64	63.18 –65.09	13.10	(0.18)	72.64	71.89 –73.90	14.64	(0.16)	72.84	71.65 –73.12	14.78	(0.15)
Cu	8.46	7.99 – 8.67	2.91	(0.09)	4.53	4.12 – 4.65	1.56	(0.07)	3.16	2.96 – 3.25	1.09	(0.05)
Bi	0.00	0.00 – 0.03	0.00	(0.01)	0.19	0.06 – 0.30	0.02	(0.01)	0.10	0.02 – 0.20	0.01	(0.01)
Pb	0.00	0.00 – 0.05	0.00	(0.02)	0.00	0.00 – 0.03	0.00	(0.01)	0.10	0.05 – 0.15	0.01	(0.01)
Zn	0.03	0.00 – 0.11	0.01	(0.01)	0.03	0.01 – 0.09	0.01	(0.01)	0.00	0.00 – 0.04	0.00	(0.01)
Fe	0.03	0.00 – 0.13	0.01	(0.01)	0.00	0.00 – 0.04	0.00	(0.01)	0.03	0.01 – 0.05	0.01	(0.01)
Au	0.00	0.00 – 0.03	0.00	(0.01)	0.09	0.05 – 0.18	0.01	(0.01)	0.09	0.05 – 0.18	0.01	(0.01)
Sb	9.64	9.11 –10.00	1.73	(0.07)	0.06	0.02 – 0.12	0.01	(0.01)	0.45	0.29 – 0.59	0.08	(0.03)
As	0.59	0.21 – 0.71	0.17	(0.04)	6.06	5.88 – 6.15	1.77	(0.07)	5.99	5.41 – 6.23	1.75	(0.08)
S	16.23	15.88 –16.53	11.06	(0.12)	16.15	15.94 –16.37	10.96	(0.13)	16.46	16.01 –16.74	11.23	(0.10)
Se	0.00	0.00 – 0.03	0.00	(0.01)	0.04	0.00 – 0.08	0.01	(0.01)	0.00	0.00 – 0.02	0.00	(0.01)
Te	0.06	0.01 – 0.14	0.00	(0.02)	0.06	0.03 – 0.14	0.01	(0.01)	0.18	0.08 – 0.25	0.03	(0.01)
Total	99.68	99.12– 100.87	29.00		99.85	99.25– 101.06	29.00		99.40	99.07– 100.95	29.00	

The ratio of atoms is calculated on the basis of 29 atoms.

Lorentz-polarization correction were performed with the Bruker–Nonius EvalCCD program package. Subsequent calculations were conducted with the Jana2000 program suite (Petříček & Dušek 2000), except for the optimization of the crystal shape and dimension, which were performed with X-shape (Stoe & Cie 1996), based on the Habitus program (Herrendorf 1993), and the structure drawings, which were made with the program Diamond (Brandenburg 2001). Full-matrix refinements were carried out on F^2, with all reflections included. Tables of structure factors for these minerals are available from the Depository of Unpublished Data on the MAC web site [*e.g.*, document antimonpearceite CM45_321].

Antimonpearceite

The study of the antimonpearceite crystal was made slightly above room temperature (*i.e.,* 330 K) to get rid of visible diffuse lines related to the proximity of a phase transition occurring just below 300 K (Bindi *et al.* 2006b). The high temperature was achieved by means of an Oxford cryostream cooler. The diffraction pattern was found to be consistent with trigonal symmetry, with $a \approx 7.5$ and $c \approx 11.9$ Å. The sets of reflections were corrected for absorption with a Gaussian analytical method and averaged according to the point group $\bar{3}m1$ ($R_{int} = 0.0358$). Starting from the model obtained for the structure of pearceite (Bindi *et al.* 2006a), the refinement in the $P\bar{3}m1$ space group converged smoothly to a residual R of 0.0352. To mimic the spread of electrons associated with silver along diffusion paths, up to fourth-order non-harmonic Gram–Charlier tensors were used for the Debye–Waller description (Johnson & Levy 1974, Kuhs 1984). Crystal characteristics, data collection and reduction parameters, and results of the refinement are given in Table 3. Atom parameters are reported in Tables 4, 5, and 6.

Arsenpolybasite-222

The diffraction pattern of the arsenpolybasite-222 crystal is apparently consistent with a trigonal symmetry, with the *a* and *c* parameters doubled ($a \approx 15.0$, $c \approx 24.0$ Å) compared to those of pearceite ($a \approx 7.4$, $c \approx 11.8$ Å; Bindi *et al.* 2006a). However, taking into account the findings of Evain *et al.* (2006a) obtained for the structure of polybasite-222, after the correction for absorption by adopting a Gaussian analytical method, the reflection dataset was transformed in the *C*-centered orthohexagonal cell and averaged accordingly, taking into account the twin law that makes the twin lattice ($\mathbf{L}_T$) hexagonal [twinning by metric merohedry: Nespolo (2004) and references therein]. It is worth noting that the only equivalent reflections of the twinned crystal are those related by the inversion operation, as {E} and {i} are the only classes of 2/*m* that are complete classes of the first-degree twin polychromatic point-group (Nespolo 2004):

$$\kappa_{WB}^{(3)} = \left(\bar{3}^{(3)} \frac{2^{(2,1)}}{m^{2,1}} \right)^{(3)}$$

In the previous polychromatic symbol, elements that do not act as twin elements (achromatic elements) are indicated without chromatic index (none in the present case), those that exchange all the individuals have one chromatic index [(3) in the present case], and finally those with partial chromaticity, which exchange a subset of the individuals and leave the other unchanged, are indicated with two chromatic indices [(2,1) in the

TABLE 3. CRYSTALLOGRAPHIC DATA FOR THE CRYSTALS SELECTED

	antimonpearceite	arsenpolybasite-221	arsenpolybasite-222
Crystal data			
Chemical formula	$Ag_{12.89}Cu_{3.11}Sb_{1.89}As_{0.11}S_{11}$	$Ag_{14.52}Cu_{1.48}As_2S_{11}$	$Ag_{14.89}Cu_{1.11}As_{1.88}Sb_{0.12}S_{11}$
Temperature (K)	330	300	300
Mol. wt. ($g.mol^{-1}$)	2179	2163	2185
Space group	$P\bar{3}m1$	$P321$	$C2/c$
Cell parameters			
a (Å)	7.4805(5)	14.9746(17)	26.036(2) ($\sqrt{3}b$)
b (Å)			15.0319(13)
c (Å)	11.8836(13)	11.9982(6)	24.042(3)
β (°)			90.000(13)
V ($Å^3$)	575.89(8)	2330.0(4)	9409.5(15)
Z	1	4	16
Density, calc. ($g.cm^{-3}$)	6.282	6.164	6.167
Crystal color	black	black	black
Crystal shape	block	block	block
Crystal size (mm)	0.08 × 0.12 × 0.18	0.10 × 0.11 × 0.16	0.07 × 0.08 × 0.13

Data collection

Diffractometer		Bruker-Nonius Kappa CCD	
Radiation		Mo K-$L_{2,3}$ (0.71073 Å)	
Monochromator		oriented graphite (002)	
Scan mode		φ / ω	
$\sin\theta / \lambda_{max}$ (Å^{-1}) / θ_{max} (°)	0.866 / 38.0	0.807 / 35.0	0.807 / 35.0
Coverage (%) at θ_{max}	98	99	99
hkl range	$-11 \le h \le 11$	$-24 \le h \le 24$	$-41 \le h \le 41$
	$-12 \le k \le 12$	$-24 \le k \le 24$	$-24 \le k \le 22$
	$-18 \le l \le 20$	$-19 \le l \le 19$	$-38 \le l \le 38$
No. of reflections	8883	81381	103848

Data reduction

Linear absorption coefficient (mm^{-1})	16.773	17.009	16.798
Absorption correction		Gaussian integration method	
T_{min}/T_{max}	0.100/0.252	0.157/0.401	0.263/ 0.370
No. of independent reflections	1216	6805	32542
Criterion for obs. refl.		$I > 2\sigma(I)$	
No. of observed reflections	1095	4639	22008
R_{int}	0.0358	0.0674	0.0640
Polychromatic point group for first-degree twin		$\kappa^{(4)} = \left(\frac{6^{(2)}2^{(2)}2^{(2)}}{m^{(2)}m^{(2)}m^{(2)}}\right)^{(4)}$	$\kappa_{WB}{}^{(3)} = \left(\overline{3}^{(3)}\frac{2^{(2,1)}}{m^{2,1}}\right)^{(3)}$
Twin matrices		$\begin{bmatrix}1&0&0\\0&1&0\\0&0&1\end{bmatrix}$, $\begin{bmatrix}-1&0&0\\0&-1&0\\0&0&-1\end{bmatrix}$, $\begin{bmatrix}1&0&0\\0&1&0\\0&0&1\end{bmatrix}$, $\begin{bmatrix}-\frac{1}{2}&\frac{1}{2}&0\\-\frac{3}{2}&-\frac{1}{2}&0\\0&0&1\end{bmatrix}$, $\begin{bmatrix}1&-1&0\\0&-1&0\\0&0&-1\end{bmatrix}$, $\begin{bmatrix}-1&1&0\\0&1&0\\0&0&1\end{bmatrix}$, $\begin{bmatrix}-\frac{1}{2}&-\frac{1}{2}&0\\\frac{3}{2}&-\frac{1}{2}&0\\0&0&1\end{bmatrix}$	
Twin-volume fractions		0.17(5), 0.21(3), 0.31(3), 0.31(3)	0.8088(9), 0.1132(7), 0.0780(8)

Refinement

Refinement coeff.		F^2	
F(000)	973	3869	15621
No. of reflections in refinement	1216	5465	32542
No. of observed reflections	1095	4639	22008
No. of refined parameters	98	186	552
Weighting scheme		$w = 1 / [\sigma^2(I) + (0.044 \times I)^2]$	
$R^\dagger$ (obs) / $R^\dagger$ (all)	0.0352 / 0.0410	0.0426 / 0.061	0.0716 / 0.1216
$wR^{2\dagger}$ (obs) / $wR^{2\dagger}$ (all)	0.1115 / 0.1170	0.0898 / 0.0974	0.1441 / 0.1669
S (obs) / S (all)	2.11 / 2.09	1.33 / 1.33	1.63 / 1.72
Secondary ext. coeff.‡	0.13(4)	0.24(2)	none
Diff. Fourier (e-/Å^3)	[-0.93, 1.26]	[-1.10,1.09]	[-2.56, 2.72]

† $R = \Sigma||F_o| - |F_c|| / \Sigma|F_o|$. $wR^2 = [\Sigma\, w\,(|F_o|^2 - |F_c|^2)^2 / \Sigma\, w\,(|F_o|^4)]^{1/2}$.

‡ Isotropic secondary extinction, Type I -- Gaussian distribution (Becker & Coppens 1974).

present case]. Finally, the global chromaticity, which indicates the number of individuals (3 in the present case), is given as an external index. In our case, 2/*m* is thus the eigensymmetry of the individual.

Starting from the atom coordinates of polybasite-222 (Evain *et al*. 2006a), the refinement in space group *C*2/*c* smoothly converged to $R = 0.112$ for observed reflections [$2\sigma(I)$ level], including all the collected reflections in the refinement. At this point, the introduction of an additional twin-law with a two-fold axis, perpendicular to the previous three-fold axis, was tested as a generator twin-element, as it was used in the structure determination of polybasite-222 (Evain *et al*. 2006a). It did not give significant twin-volume ratios, and the additional twin-law was removed from the model.

A non-harmonic approach with a Gram–Charlier development of the Debye–Waller factor up to the third order (Johnson & Levy 1974, Kuhs 1984) was then used to properly describe the electron density of two Ag atoms (*i.e.,* Ag5, Ag9), in the vicinity of which residues were found in the difference-Fourier synthesis maps. At the last stage, with anisotropic atom-displacement parameters for all atoms and no constraints other than full site-occupancy, the residual value settled at $R = 0.0716$ (Rw = 0.1441) for 22008 independent observed reflections [$2\sigma(I)$ level] and 552 parameters and at $R = 0.1216$ (Rw = 0.1669) for all 32542 independent reflections. Crystal characteristics, data collection and reduction parameters, and refinement results are given in Table 3. Atom parameters are reported in Tables 4, 5, and 6.

Arsenpolybasite-221

As for the arsenpolybasite-222, the arsenpolybasite-221 crystal system seems to be trigonal and could be indexed with a hexagonal cell ($a \approx 15.0$, $c \approx 12.0$ Å) related to that of antimonpearceite by the $2a \times 2b \times c$ relationship. After the usual Lorentz–polarization adjustment and a Gaussian analytical absorption-correction based upon optimized shape and dimension of the crystal, the structure refinement was carried out in space group *P*321 starting from the atom coordinates of polybasite-221 (Evain *et al*. 2006a). In this space group and after the introduction of a mirror twin-operation (first-degree twin, $\bar{6}'2m'$ Shubnikov $K^{(2)}$ dichromatic point-group), the refinement smoothly converged toward a residual $R = 0.0434$ value. The results are then only slightly improved ($R = 0.0426$) by the adjunction of the inversion twin-operation, yielding the following polychromatic point-group (Nespolo 2004):

$$\kappa^{(4)} = \left(\frac{6^{(2)}2^{(2)}2^{(2)}}{m^{(2)}m^{(2)}m^{(2)}} \right)^{(4)}$$

Crystal characteristics, data collection and reduction parameters, and refinement results are gathered in Table 3. Atom parameters are reported in Tables 4, 5, and 6.

TABLE 4a. SITE-OCCUPANCY FACTORS, FRACTIONAL COORDINATES, AND EQUIVALENT ISOTROPIC DISPLACEMENT PARAMETERS (Å²) OF ATOMS IN ANTIMONPEARCEITE, WITH STANDARD UNCERTAINTIES

Atom	*s.o.f.*	*x*	*y*	*z*	U_{eq}
Sb	0.923(16)	0.6667	0.3333	0.41180(4)	0.02462(15)
As	0.077	0.6667	0.3333	0.41180	0.02462
Ag1	0.66(2)	0.14879(15)	0.2976(3)	0.38289(16)	0.0584(7)
Cu1	0.34	0.14879	0.2976	0.38289	0.0584
Ag2	0.411(5)	0.196(4)	0.3651(7)	0.1206(3)	0.461(11)
Ag3	0.339(5)	0.3740(8)	0.2792(13)	0.1168(4)	0.120(3)
Cu2	1	0	0	0	0.0314(3)
S1	1	0	0	0.18171(13)	0.0288(4)
S2	1	0.50432(7)	0.00864(14)	0.31065(10)	0.0301(3)
S3	1	0.3333	0.6667	0.0153(2)	0.0448(6)
S4	0.1667	0	0.0798(7)	0.5	0.0334(13)

Description of the Structures

Basically, although not layered compounds, the structures of antimonpearceite, arsenpolybasite-221 and -222 can be easily described as a regular alternation of two kinds of layers stacked along [001]: a first layer (labeled A or A') with general composition $[(Ag,Cu)_6(As,Sb)_2S_7]^{2-}$, and a second layer (labeled B or B'), with general composition $[Ag_9CuS_4]^{2+}$.

Antimonpearceite

In the crystal structure of antimonpearceite (Fig. 1), (Sb,As) forms (Sb,As)S_3 pyramids, as typically occur in

TABLE 4b. SITE-OCCUPANCY FACTORS, FRACTIONAL COORDINATES, AND EQUIVALENT ISOTROPIC DISPLACEMENT PARAMETERS (Å²) OF ATOMS IN ARSENPOLYBASITE-221, WITH STANDARD UNCERTAINTIES

Atom	*s.o.f.*	*x*	*y*	*z*	U_{eq}
As1	1	0.3333	0.6667	0.09980(15)	0.0204(4)
As2	1	0.33359(8)	0.16003(7)	0.09832(8)	0.0189(3)
Ag1	1	0.36371(7)	0.42908(9)	0.10401(8)	0.0389(4)
Ag2	0.813(16)	0.09037(9)	0.42152(11)	0.13506(10)	0.0500(5)
Cu2'	0.187(16)	0.0904	0.4215	0.1351	0.0500(5)
Ag3	0.869(17)	0.07803(11)	0.15006(13)	0.11754(11)	0.0569(8)
Cu3'	0.131(17)	0.078	0.1501	0.1175	0.0569(8)
Ag4	1	0.57112(10)	0.41821(10)	0.11501(10)	0.0506(5)
Ag5	1	0.34634(8)	0.54688(8)	0.39198(9)	0.0446(4)
Ag6	1	0.26987(12)	0.06958(9)	0.39070(9)	0.0580(6)
Ag7	1	0.13407(11)	0.17634(9)	0.37296(10)	0.0574(6)
Ag8	1	0.52522(15)	0.16860(10)	0.37615(9)	0.0695(7)
Ag9	1	0.10038(8)	0.42134(8)	0.39254(9)	0.0448(5)
Ag10	1	0.38282(16)	0.30734(8)	0.36580(8)	0.0875(8)
Cu1	1	0	0.51201(12)	0.5	0.0251(6)
Cu2	1	0	0	0.5	0.0331(11)
S1	1	0.2715(2)	0.5150(2)	0.1906(2)	0.0238(10)
S2	1	-0.01023(18)	0.2402(2)	0.1981(2)	0.0264(10)
S3	1	0.2618(3)	0.2468(3)	0.1777(2)	0.0266(11)
S4	1	0.4839(2)	0.2415(2)	0.1922(2)	0.0267(10)
S5	1	0.4938(2)	0.50125(18)	0.32031(18)	0.0226(9)
S6	1	0	0	0.3201(4)	0.0237(12)
S7	1	0.1953(2)	0.3430(2)	0.46279(19)	0.0274(10)
S8	1	0.3333	0.6667	0.5393(4)	0.0306(13)
S9	1	0.5324(3)	0.5324(3)	0	0.0529(18)
S10	0.3333	0.0248(11)	0.0248(11)	0	0.070(7)

sulfosalts, and copper links two sulfur atoms in a linear coordination. The silver cations are found in a fully occupied position, labeled Ag1,Cu1, and in other two sites corresponding to the most pronounced probability density-function (pdf) locations (modes) of diffusion-like paths (*i.e.*, Ag2 and Ag3). These positions correspond to low-coordination sites, in agreement with the preference of silver for such environments (Table 7).

In the A layer of the crystal structure of antimonpearceite, there occurs the only fully occupied position for the silver atoms. This fully occupied position, labeled (Ag1,Cu1), is triangularly coordinated by S atoms (two S2 and one S4), showing bond distances ranging from 2.464(2) to 2.465(2) Å, if the splitting of the S4 position is neglected in the calculation [see Bindi *et al.* (2006a) for an extensive description of the disorder]. The average bond-distance, 2.465 Å, is in agreement with a partial substitution of copper for silver at this site. The (Sb,As)S_3 trigonal pyramids are isolated from

TABLE 4c. SITE-OCCUPANCY FACTORS, FRACTIONAL COORDINATES, AND EQUIVALENT ISOTROPIC DISPLACEMENT PARAMETERS (Å^2) OF ATOMS IN ARSENPOLYBASITE-222, WITH STANDARD UNCERTAINTIES

Atom	*s.o.f.*	*x*	*y*	*z*	U_{eq}
As1	0.930(8)	0.16645(3)	0.24708(6)	0.04970(3)	0.0195(2)
Sb1'	0.070	0.16645	0.24708	0.04970	0.0195
As2	0.931(8)	0.16620(4)	0.75572(6)	0.05088(3)	0.0200(2)
Sb2'	0.069	0.16620	0.75572	0.05088	0.0200
As3	0.901(10)	0.41985(3)	-0.00414(6)	0.05004(4)	0.0198(2)
Sb3'	0.099	0.41985	-0.00414	0.05004	0.0198
As4	1	0.41230(3)	0.49968(6)	0.05034(4)	0.0175(2)
Sb4'	0	0.41230	0.49968	0.05034	0.0175
Ag1	1	0.03356(3)	0.14478(7)	0.05354(4)	0.0407(3)
Ag2	1	0.04409(3)	0.36395(8)	0.06653(5)	0.0479(3)
Ag3	0.916(13)	0.04448(4)	0.62225(9)	0.06430(5)	0.0604(5)
Cu3'	0.084	0.04458	0.62225	0.06430	0.0604
Ag4	1	0.03192(3)	0.85960(7)	0.05493(4)	0.0417(3)
Ag5	0.929(13)	0.16076(9)	0.00213(12)	0.06933(9)	0.0505(4)
Cu5'	0.071	0.16076	0.00213	0.06933	0.0505
Ag6	1	0.18442(3)	0.49998(6)	0.05078(4)	0.0352(2)
Ag7	1	0.28741(3)	0.10329(6)	0.05266(4)	0.0383(3)
Ag8	1	0.28577(4)	0.37499(7)	0.06294(4)	0.0457(3)
Ag9	0.941(13)	0.29077(8)	0.63252(16)	0.06172(9)	0.0596(5)
Cu9'	0.059	0.29077	0.63252	0.06172	0.0596
Ag10	1	0.28734(3)	0.89735(7)	0.05653(4)	0.0402(3)
Ag11	1	0.42857(4)	0.25102(6)	0.05590(5)	0.0473(3)
Ag12	1	0.41678(6)	0.74641(7)	0.06010(5)	0.0657(5)
Ag13	1	0.16044(3)	0.00663(7)	0.19801(4)	0.0459(3)
Ag14	1	0.34579(4)	0.02325(13)	0.18229(5)	0.0859(6)
Ag15	1	0.46263(4)	0.00806(8)	0.19693(4)	0.0495(3)
Ag16	1	0.09995(4)	0.19356(8)	0.19867(4)	0.0472(3)
Ag17	1	0.22640(4)	0.17523(7)	0.19588(4)	0.0452(3)
Ag18	1	0.41216(3)	0.20300(9)	0.18558(4)	0.0540(4)
Ag19	1	0.05164(4)	0.37683(6)	0.19673(4)	0.0409(3)
Ag20	1	0.17326(4)	0.37439(7)	0.19283(4)	0.0437(3)
Ag21	1	0.28943(4)	0.36069(7)	0.19433(4)	0.0460(3)
Ag22	1	0.39990(4)	0.41778(9)	0.19354(4)	0.0574(4)
Ag23	1	0.06335(4)	0.63587(7)	0.18914(5)	0.0531(3)
Ag24	1	0.18965(6)	0.63290(9)	0.18610(4)	0.0699(4)
Ag25	1	0.31689(6)	0.60230(9)	0.19004(5)	0.0700(4)
Ag26	1	0.46399(6)	0.59426(8)	0.18455(5)	0.0758(5)
Ag27	1	0.01927(5)	0.90582(7)	0.18457(5)	0.0574(4)
Ag28	1	0.13125(6)	0.81215(8)	0.19650(4)	0.0614(4)
Ag29	1	0.25823(7)	0.84371(9)	0.19034(5)	0.0812(5)
Ag30	1	0.41478(3)	0.80609(10)	0.18661(4)	0.0559(4)
Cu1	1	0	0.23864(12)	0.25	0.0235(4)
Cu2	1	0	0.75232(15)	0.25	0.0327(5)
Cu3	1	0.24348(4)	0.50459(9)	0.24966(5)	0.0242(3)
S1	1	0.12189(8)	0.14351(15)	0.09778(10)	0.0231(6)
S2	1	0.13555(8)	0.37008(14)	0.09207(10)	0.0218(5)
S3	1	0.24279(8)	0.23817(15)	0.09531(10)	0.0220(6)
S4	1	0.13607(8)	0.63134(15)	0.09189(10)	0.0234(6)
S5	1	0.12198(8)	0.85957(15)	0.10001(9)	0.0222(6)
S6	1	0.24214(8)	0.75954(15)	0.09680(10)	0.0241(6)
S7	1	0.49319(8)	-0.00210(16)	0.10211(9)	0.0230(5)
S8	1	0.37853(8)	0.11319(15)	0.08794(10)	0.0232(6)
S9	1	0.37997(9)	0.38082(15)	0.09695(10)	0.0246(6)
S10	1	0.49259(8)	0.50245(16)	0.08778(10)	0.0233(5)
S11	1	0.38047(8)	0.61128(16)	0.10335(10)	0.0247(6)
S12	1	0.37612(9)	0.88934(15)	0.09639(10)	0.0246(6)
S13	1	0.23004(9)	-0.0038(2)	-0.00040(11)	0.0361(8)
S14	1	0.49211(16)	0.7730(2)	0.00161(13)	0.0529(11)
S15	1	0.07378(8)	0.01467(17)	0.23222(10)	0.0270(6)
S16	1	0.24874(8)	0.00795(17)	0.16090(9)	0.0228(5)
S17	1	0.00330(9)	0.24723(16)	0.16047(8)	0.0223(5)
S18	1	0.32881(9)	0.22833(16)	0.22997(10)	0.0262(6)
S19	1	0.09980(9)	0.50260(16)	0.23060(10)	0.0253(6)
S20	1	0.24643(8)	0.49580(15)	0.15991(8)	0.0214(5)
S21	1	0.00032(9)	0.74878(16)	0.16020(8)	0.0228(6)
S22	1	0.33248(10)	0.75324(19)	0.23170(10)	0.0291(6)

TABLE 5a. ANISOTROPIC DISPLACEMENT PARAMETERS U_{ij} (Å^2) AND STANDARD UNCERTAINTIES FOR THE CRYSTAL OF ANTIMONPEARCEITE

Atom	U_{11}	U_{22}	U_{33}	U_{12}	U_{13}	U_{23}
Sb	0.02671(19)	0.02671(19)	0.0205(2)	0.01335(10)	0	0
As	0.02671	0.02671	0.0205	0.01335	0	0
Ag1	0.0457(8)	0.0728(10)	0.0658(11)	0.0364(5)	-0.0022(3)	-0.0045(6)
Cu1	0.0457	0.0728	0.0658	0.0364	-0.0022	-0.0045
Ag2	0.84(3)	0.0507(9)	0.0482(8)	-0.111(4)	-0.019(4)	0.0059(6)
Ag3	0.086(3)	0.197(6)	0.056(2)	0.055(3)	-0.0025(17)	-0.046(2)
Cu2	0.0392(4)	0.0392(4)	0.0158(4)	0.0196(2)	0	0
S1	0.0354(5)	0.0354(5)	0.0157(5)	0.0177(2)	0	0
S2	0.0297(3)	0.0223(4)	0.0358(5)	0.01113(18)	-0.00027(15)	-0.0005(3)
S3	0.0454(7)	0.0454(7)	0.0435(12)	0.0227(3)	0	0

TABLE 5b. ANISOTROPIC DISPLACEMENT PARAMETERS U_{ij} (Å^2) AND STANDARD UNCERTAINTIES FOR THE CRYSTAL OF ARSENPOLYBASITE-221

Atom	U_{11}	U_{22}	U_{33}	U_{12}	U_{13}	U_{23}
As1	0.0218(5)	0.0218(5)	0.0175(7)	0.0109(3)	0	0
As2	0.0201(5)	0.0195(4)	0.0166(3)	0.0096(4)	0.0007(4)	-0.0001(3)
Ag1	0.0413(4)	0.0360(5)	0.0419(4)	0.0213(4)	0.0095(4)	0.0013(5)
Ag2	0.0301(7)	0.0439(7)	0.0561(7)	0.0035(5)	-0.0111(5)	0.0027(5)
Cu2'	0.0301(7)	0.0439(7)	0.0561(7)	0.0035(5)	-0.0111(5)	0.0027(5)
Ag3	0.0440(8)	0.0753(11)	0.0617(9)	0.0376(8)	0.0039(6)	0.0053(7)
Cu3'	0.0440(8)	0.0753(11)	0.0617(9)	0.0376(8)	0.0039(6)	0.0053(7)
Ag4	0.0427(6)	0.0389(5)	0.0534(6)	0.0079(5)	-0.0022(5)	0.0038(5)
Ag5	0.0425(5)	0.0531(6)	0.0407(5)	0.0259(4)	-0.0029(4)	-0.0121(5)
Ag6	0.0954(10)	0.0504(6)	0.0362(5)	0.0424(7)	-0.0137(6)	-0.0116(4)
Ag7	0.0787(9)	0.0273(5)	0.0490(6)	0.0137(5)	-0.0193(6)	-0.0020(5)
Ag8	0.1253(12)	0.0327(6)	0.0400(5)	0.0316(7)	-0.0082(7)	0.0020(5)
Ag9	0.0574(6)	0.0471(5)	0.0497(5)	0.0410(5)	-0.0171(5)	-0.0108(5)
Ag10	0.1442(15)	0.0266(5)	0.0342(4)	-0.0004(7)	0.0055(8)	0.0026(4)
Cu1	0.0306(11)	0.0300(6)	0.0149(6)	0.0153(6)	-0.0011(7)	-0.0006(3)
Cu2	0.0407(15)	0.0407(15)	0.0179(15)	0.0204(7)	0	0
S1	0.0215(12)	0.0208(12)	0.0303(11)	0.0115(11)	0.0012(10)	-0.0026(10)
S2	0.0157(9)	0.0278(14)	0.0301(11)	0.0068(11)	-0.0012(8)	0.0001(11)
S3	0.0281(14)	0.0273(15)	0.0305(11)	0.0184(11)	0.0010(12)	0.0001(12)
S4	0.0209(12)	0.0203(13)	0.0369(13)	0.0087(11)	-0.0037(10)	0.0021(11)
S5	0.0301(12)	0.0202(10)	0.0149(8)	0.0106(11)	0.0019(8)	-0.0006(7)
S6	0.0270(15)	0.0270(15)	0.0171(19)	0.0135(8)	0	0
S7	0.0335(12)	0.0264(13)	0.0256(10)	0.0175(12)	-0.0029(9)	-0.0016(10)
S8	0.0327(16)	0.0327(16)	0.026(2)	0.0163(8)	0	0
S9	0.0497(19)	0.0497(19)	0.0270(19)	0.001(3)	-0.0022(11)	0.0022(11)
S10	0.060(10)	0.060(10)	0.036(6)	-0.010(7)	-0.025(8)	0.025(8)

each other, but linked to (Ag1,Cu1)S_3 units to constitute a layer and not a three-dimensional structure as in $Cu_{12}Sb_4S_{13}$ (Pfitzner *et al.* 1997).

TABLE 5c. ANISOTROPIC DISPLACEMENT PARAMETERS U_{ij} (Å^2) AND STANDARD UNCERTAINTIES FOR THE CRYSTAL OF ARSENPOLYBASITE-222

Atom	U_{11}	U_{22}	U_{33}	U_{12}	U_{13}	U_{23}
As1	0.0201(4)	0.0195(4)	0.0190(4)	-0.0001(3)	-0.0004(3)	-0.0005(3)
Sb1'	0.0201	0.0195	0.0190	-0.0001	-0.0004	-0.0005
As2	0.0212(4)	0.0203(4)	0.0186(4)	0.0007(3)	-0.0008(3)	0.0006(3)
Sb2'	0.0212	0.0203(4)	0.0186	0.0007	-0.0008	0.0006
As3	0.0197(4)	0.0205(4)	0.0193(4)	-0.0002(3)	0.0009(3)	-0.0018(3)
Sb3'	0.0197	0.0205	0.0193	-0.0002	0.0009	-0.0018
As4	0.0183(3)	0.0173(4)	0.0170(3)	0.0004(3)	-0.0017(3)	-0.0004(3)
Sb4'	0.0183	0.0173	0.0170	0.0004	-0.0017	-0.0004
Ag1	0.0356(4)	0.0397(5)	0.0467(5)	-0.0062(4)	-0.0072(4)	0.0066(4)
Ag2	0.0288(4)	0.0595(6)	0.0554(6)	0.0071(4)	-0.0053(4)	0.0008(5)
Ag3	0.0402(6)	0.0766(10)	0.0644(8)	-0.0252(5)	-0.0138(5)	0.0267(6)
Cu3'	0.0402	0.0766	0.0644	-0.0252	-0.0138	0.0267
Ag4	0.0351(4)	0.0411(5)	0.0487(5)	0.0050(4)	-0.0056(4)	-0.0077(4)
Ag5	0.0714(8)	0.0252(5)	0.0552(7)	0.0014(4)	0.0295(6)	-0.0018(4)
Cu5'	0.0714	0.0252	0.0552	0.0014	0.0295	-0.0018
Ag6	0.0366(4)	0.0325(4)	0.0364(4)	-0.0004(3)	0.0116(3)	-0.0001(3)
Ag7	0.0338(4)	0.0364(4)	0.0446(5)	0.0060(3)	-0.0023(3)	-0.0097(4)
Ag8	0.0396(5)	0.0453(5)	0.0522(6)	-0.0155(4)	0.0016(4)	0.0078(4)
Ag9	0.0535(7)	0.0659(9)	0.0593(8)	0.0328(6)	-0.0106(5)	-0.0232(6)
Cu9'	0.0535	0.0659	0.0593	0.0328	-0.0106	-0.0232
Ag10	0.0327(4)	0.0389(5)	0.0490(5)	-0.0055(3)	-0.0045(4)	0.0085(4)
Ag11	0.0573(6)	0.0320(5)	0.0525(6)	-0.0028(4)	0.0034(5)	-0.0002(4)
Ag12	0.1095(11)	0.0289(5)	0.0590(7)	-0.0052(6)	0.0117(7)	0.0031(5)
Ag13	0.0216(3)	0.0657(6)	0.0506(5)	-0.0063(4)	0.0063(3)	-0.0136(5)
Ag14	0.0254(4)	0.1977(18)	0.0347(5)	-0.0119(7)	-0.0019(4)	-0.0022(8)
Ag15	0.0430(5)	0.0726(7)	0.0330(4)	0.0118(5)	0.0099(3)	0.0071(5)
Ag16	0.0474(5)	0.0522(6)	0.0421(5)	0.0072(4)	-0.0088(4)	-0.0123(4)
Ag17	0.0557(5)	0.0416(5)	0.0384(5)	-0.0002(4)	0.0116(4)	-0.0033(4)
Ag18	0.0256(4)	0.0900(9)	0.0463(6)	-0.0014(5)	0.0018(4)	0.0167(6)
Ag19	0.0511(5)	0.0263(4)	0.0452(5)	-0.0132(3)	-0.0142(4)	0.0024(3)
Ag20	0.0436(5)	0.0494(5)	0.0381(5)	-0.0033(4)	0.0008(4)	0.0091(4)
Ag21	0.0483(5)	0.0373(5)	0.0524(6)	0.0210(4)	0.0098(4)	0.0129(4)
Ag22	0.0626(6)	0.0752(8)	0.0346(5)	-0.0245(6)	0.0012(4)	-0.0111(5)
Ag23	0.0672(6)	0.0387(5)	0.0533(6)	0.0251(5)	-0.0201(5)	-0.0074(4)
Ag24	0.1107(10)	0.0665(8)	0.0323(5)	0.0576(7)	-0.0054(6)	-0.0078(5)
Ag25	0.0988(9)	0.0728(8)	0.0384(5)	-0.0557(7)	0.0152(6)	-0.0076(5)
Ag26	0.1439(13)	0.0488(6)	0.0348(5)	-0.0536(8)	-0.0087(7)	0.0062(5)
Ag27	0.0786(7)	0.0428(5)	0.0509(6)	-0.0298(5)	0.0147(5)	-0.0124(5)
Ag28	0.1067(9)	0.0421(5)	0.0354(5)	0.0098(6)	-0.0132(6)	0.0053(4)
Ag29	0.1531(14)	0.0500(7)	0.0402(6)	0.0503(8)	-0.0172(7)	-0.0109(5)
Ag30	0.0299(4)	0.0995(10)	0.0384(5)	0.0095(5)	-0.0024(4)	0.0061(5)
Cu1	0.0282(7)	0.0289(8)	0.0135(6)	0	-0.0014(6)	0
Cu2	0.0413(10)	0.0406(11)	0.0162(7)	0	0.0000(7)	0
Cu3	0.0285(5)	0.0296(6)	0.0145(4)	-0.0006(5)	0.0003(4)	0.0019(4)
S1	0.0221(9)	0.0175(9)	0.0296(11)	-0.0024(7)	0.0026(8)	-0.0004(8)
S2	0.0193(9)	0.0171(9)	0.0289(11)	0.0000(7)	0.0022(8)	0.0016(8)
S3	0.0170(9)	0.0196(9)	0.0293(11)	-0.0007(7)	0.0007(8)	-0.0006(8)
S4	0.0218(9)	0.0175(9)	0.0309(11)	-0.0017(8)	0.0004(8)	0.0012(8)
S5	0.0182(9)	0.0228(10)	0.0258(10)	0.0033(8)	0.0003(7)	0.0016(8)
S6	0.0180(9)	0.0198(10)	0.0343(12)	0.0002(7)	-0.0017(8)	-0.0021(8)
S7	0.0165(8)	0.0266(10)	0.0260(10)	0.0012(8)	-0.0004(7)	-0.0003(9)
S8	0.0230(10)	0.0159(9)	0.0308(11)	0.0020(7)	-0.0040(8)	-0.0020(8)
S9	0.0262(10)	0.0186(9)	0.0291(11)	-0.0042(8)	-0.0009(8)	0.0000(8)
S10	0.0185(8)	0.0238(10)	0.0278(10)	-0.0002(8)	0.0003(7)	0.0030(9)
S11	0.0215(9)	0.0214(10)	0.0313(12)	0.0019(8)	0.0038(8)	-0.0051(8)
S12	0.0225(10)	0.0185(9)	0.0328(12)	-0.0036(8)	-0.0029(8)	0.0047(8)
S13	0.0273(10)	0.0575(18)	0.0235(10)	-0.0035(12)	-0.0023(8)	0.0010(12)
S14	0.085(3)	0.0443(17)	0.0293(13)	0.0132(16)	-0.0044(16)	-0.0057(13)
S15	0.0200(9)	0.0350(13)	0.0260(10)	-0.0039(8)	0.0007(7)	-0.0030(9)
S16	0.0198(8)	0.0334(12)	0.0151(8)	0.0017(9)	0.0001(6)	-0.0009(8)
S17	0.0264(10)	0.0259(10)	0.0147(8)	-0.0039(9)	0.0021(7)	0.0004(8)
S18	0.0265(10)	0.0268(11)	0.0254(10)	0.0057(8)	0.0016(8)	0.0038(8)
S19	0.0303(10)	0.0217(9)	0.0239(9)	-0.0017(9)	-0.0010(8)	0.0002(9)
S20	0.0284(9)	0.0210(9)	0.0150(8)	0.0020(8)	-0.0006(7)	0.0001(8)
S21	0.0245(10)	0.0241(10)	0.0196(9)	0.0014(8)	-0.0024(8)	0.0014(8)
S22	0.0312(11)	0.0317(12)	0.0244(10)	-0.0040(10)	0.0004(9)	0.0002(9)

The coordinations of the other silver positions are similar to those reported for the crystal structure of pearceite (Bindi *et al.* 2006a). Note that the Cu2 position shows a linear coordination with two distances at 2.158(1) Å. Although these values are shorter than that found by the sum of ionic radii (*i.e.,* 2.30 Å: Shannon 1981), they are in perfect agreement with those found in KCuS (2.129 and 2.162 Å: Savelsberg & Schäfer 1978), in which Cu2 shows a similar linear coordination with sulfur, which was explained through band-structure calculations by Gaudin *et al.* (2001).

Arsenpolybasite-222

The crystal structure of arsenpolybasite-222 (Fig. 2) can be seen as a succession along the *c* axis of two module layers: the $[(Ag,Cu)_6Sb_2S_7]^{2-}$ A (or A') module layer and the $[Ag_9CuS_4]^{2+}$ B (or B') module layer (A,B and A',B' being related by a *c* glide mirror operation of symmetry).

In the $[(Ag,Cu)_6Sb_2S_7]^{2-}$ A (or A') module layer, each silver cation has a three-fold coordination with sulfur. Out of the 12 independent Ag atoms of the A module layer, Ag3, Ag5 and Ag9 exhibit shorter <Ag–S> distances (2.460, 2.465 and 2.498 Å, respectively). This structural feature indicates a partial replacement of silver by copper at these particular sites. In the $[AsS_3]^{3-}$ pyramids, the overall mean As–S bond distance [2.266 Å] is consistent with the value observed in the crystal structure of proustite, $Ag_3[AsS_3]$ (2.293 Å, Engel & Nowacki 1966).

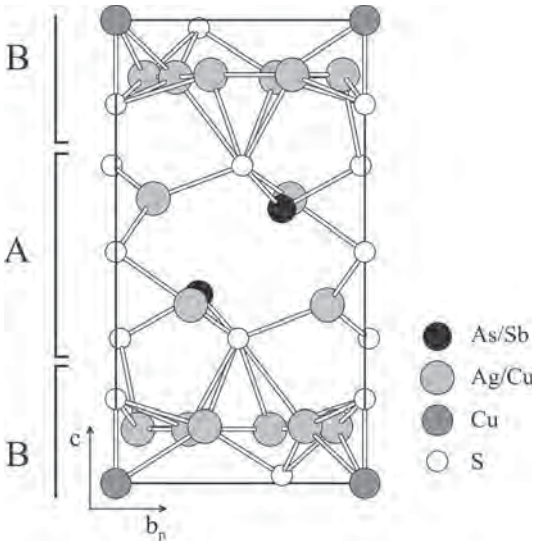

FIG. 1. Projection of the antimonpearceite structure along the *a* axis (hexagonal symmetry), emphasizing the succession of the $[(Ag,Cu)_6Sb_2S_7]^{2-}$ A (A') and $[Ag_9CuS_4]^{2+}$ B (B') module layers.

TABLE 6. HIGHER-ORDER DISPLACEMENT PARAMETERS AND STANDARD UNCERTAINTIES †‡ FOR THE CRYSTALS SELECTED

	antimonpearceite				antimonpearceite			arsenpolybasite-222	
	Ag1,Cu1	Ag2	Ag3		Ag1,Cu1	Ag3		Ag5,Cu5'	Ag9,Cu9'
C^{111}	-0.0002(5)	-3.1(2)	0.015(6)	D^{1111}	-0.0024(7)	0.075(9)	C^{111}	-0.00056(4)	0.00030(3)
C^{112}	0.0064(5)	0.50(4)	0.061(8)	D^{1112}	-0.0020(5)	0.093(11)	C^{112}	-0.00004(3)	0.00081(4)
C^{113}	0.00009(18)	-0.004(12)	-0.0054(13)	D^{1113}	0.00142(18)	-0.0062(18)	C^{113}	-0.00048(2)	-0.00034(2)
C^{122}	0.0197(17)	-0.111(9)	0.060(14)	D^{1122}	-0.0020(5)	0.119(16)	C^{122}	0.00022(3)	0.00188(8)
C^{123}	-0.0020(2)	-0.012(3)	-0.011(2)	D^{1123}	0.00188(16)	-0.012(3)	C^{123}	-0.00006(2)	-0.00069(3)
C^{133}	0.00126(10)	0.002(3)	0.0016(5)	D^{1133}	-0.00081(10)	0.0018(5)	C^{133}	-0.00036(2)	0.00021(2)
C^{222}	0.039(3)	0.025(2)	0.04(3)	D^{1222}	-0.0022(17)	0.22(3)	C^{222}	0.00023(9)	0.0038(2)
C^{223}	-0.0040(4)	0.0041(6)	-0.028(4)	D^{1223}	0.0028(6)	-0.032(4)	C^{223}	0.00002(4)	-0.00152(8)
C^{233}	0.0025(2)	0.0001(4)	0.0050(10)	D^{1233}	-0.00121(10)	0.0049(7)	C^{233}	0.00000(3)	0.00046(5)
C^{333}	-0.0037(2)	-0.0011(3)	-0.0005(4)	D^{1333}	0.00058(7)	-0.0006(2)	C^{333}	-0.00031(4)	-0.00011(4)
				D^{2222}	-0.004(3)	0.12(4)			
				D^{2223}	0.0056(12)	0.010(7)			
				D^{2233}	-0.0024(2)	-0.0091(16)			
				D^{2333}	0.00116(14)	0.0022(4)			
				D^{3333}	0.00013(14)	-0.00036(18)			

† Third-order tensor elements C^{ijk} are multiplied by 10^3. ‡ Fourth-order tensor elements D^{ijkl} are multiplied by 10^4.

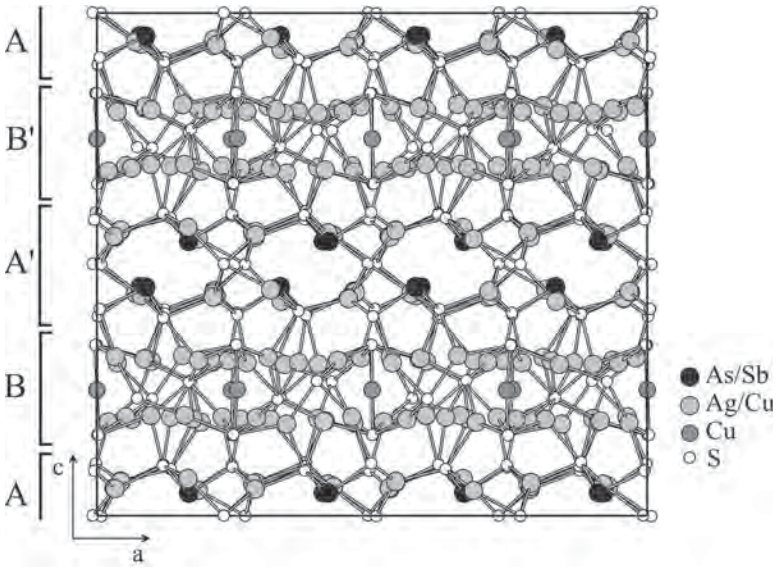

FIG. 2. Projection of the arsenpolybasite-222 structure along the *b* axis (monoclinic symmetry), emphasizing the succession of the $[(Ag,Cu)_6Sb_2S_7]^{2-}$ A (A') and $[Ag_9CuS_4]^{2+}$ B (B') module layers.

In the $[Ag_9CuS_4]^{2+}$ B (or B') module layer, the 18 independent Ag atoms adopt various coordinations extending from quasi-linear to quasi-tetrahedral (Table 8). In detail, seven silver atoms (*i.e.*, Ag13, Ag15, Ag19, Ag21, Ag22, Ag23 and Ag28) can be considered in linear coordination with an overall mean Ag–S of 2.43 Å, although the S–Ag–S angles invariably depart from 180°. Six Ag atoms (*i.e.*, Ag18, Ag24, Ag25 Ag27, Ag29, and Ag30) may be considered as three-fold coordinated, even though some of them are in an environment of two short bonds + one long bond (Table 8). Taking into account three bonds per atom, an overall mean Ag–S of 2.59 Å can be calculated, in good agreement with both that found for the Ag(1) position in the crystal structure of stephanite, $Ag_5[SlSbS_3]$ (2.54 Å: Ribár & Nowacki 1970) and that found for the Ag position in the crystal structure of pyrargyrite, $Ag_3[SbS_3]$ (2.573 Å: Engel & Nowacki 1966). The last five silver atoms (*i.e.*, Ag14, Ag16, Ag17, Ag20, Ag26) adopt a close-to-tetrahedral coordination. Once again, taking only four bonds for the averaging, one calculates an overall mean Ag–S = 2.71 Å, which matches that found for the Ag(3) position in the crystal structure of stephanite, $Ag_5[SlSbS_3]$ (2.68 Å: Ribár & Nowacki 1970). Finally, the three copper atoms exhibit a nearly perfect linear coordination, with similar Cu–S distances [overall mean Cu–S = 2.159 Å]. The shortest cation–cation distances are: Ag–Cu: 2.7861(16) Å, Ag–Ag: 3.0016(15) Å, Ag–As : 3.377(2) Å.

Arsenpolybasite-221

The structure of 221-polybasite (Fig. 3) is obtained from the 222-polybasite structure by selecting half its cell content along the *c* axis, that is, either the A–B (or A'–B') double-module layer or the A/2–B–A'/2 (or A'/2–B'–A/2) double-module layer, since A and A' approximately correspond to each other by a ½ translation along the *c* axis.

The observed metal–sulfur distances compare well with those obtained for the 222-polybasite structure (Tables 8, 9). For instance, $\langle As–S\rangle_{221}$ = 2.264 Å matches the $\langle As–S\rangle_{222}$ = 2.266 Å value. Similarly, in the $[Ag_9CuS_4]^{2+}$ B module layer, $\langle Cu–S\rangle_{221}$ = 2.161 Å is equivalent to $\langle Cu–S\rangle_{222}$ = 2.159 Å. We also found two silver atoms (*i.e.*, Ag6 and Ag9) in a quasi-linear coordination [$\langle Ag–S\rangle_{221}$ = 2.43 Å *versus* $\langle Ag–S\rangle_{222}$

TABLE 7. THE MAIN INTERATOMIC DISTANCES (Å) AND STANDARD UNCERTAINTIES FOR THE CRYSTAL OF ANTIMONPEARCEITE SELECTED

Sb	- S2	2.423(1)	Cu2	- S1	2.158(1)	Ag1,Cu	- S2	2.464(2)
	- S2	2.423(1)		- S1	2.158(1)		- S2	2.4645(14)
	- S2	2.423(1)	<Cu2-S>		2.158		- S4‡	2.465(2)
<Sb-S>		2.423				<Ag1,Cu-S>		2.465
Ag2	- S3	2.318(5)	Ag3	- S3	2.560(6)			
	- S1	2.480(4)		- S1	2.624(5)			
	- Cu2	2.769(4)		- S2	2.705(6)			
				- Cu2	2.870(5)			

Note: ‡ values calculated with S4 in the (0,0,½) average position.

TABLE 8. THE MAIN INTERATOMIC DISTANCES (Å) AND STANDARD UNCERTAINTIES FOR THE CRYSTAL OF ARSENPOLYBASITE-222 SELECTED

$[(Ag,Cu)_6(As,Sb)_2S_7]^{2-}$ A (A') layer

As1	- S2	2.259(2)	As2	- S4	2.255(2)			
	- S1	2.260(2)		- S5	2.271(2)			
	- S3	2.274(2)		- S6	2.265(2)			
<As1-S>		2.264	<As2-S>		2.264			
As3	- S8	2.258(2)	As4	- S11	2.264(3)			
	- S12	2.259(2)		- S9	2.271(2)			
	- S7	2.283(2)		- S10	2.276(2)			
<As1-S>		2.267	<As1-S>		2.270			
Ag1	- S1	2.534(2)	Ag2	- S2	2.461(2)	Ag3,Cu	- S14	2.429(4)
	- S10	2.528(3)		- S14	2.477(4)		- S7	2.471(3)
	- S14	2.538(4)		- S7	2.558(3)		- S4	2.479(2)
<Ag1-S>		2.533	<Ag2-S>		2.499	<Ag3,Cu-S>		2.460
Ag4	- S14	2.492(4)	Ag5,Cu	- S1	2.451(3)	Ag6	- S2	2.533(2)
	- S10	2.507(3)		- S13	2.464(3)		- S13	2.536(3)
	- S5	2.583(2)		- S5	2.481(3)		- S4	2.542(2)
<Ag4-S>		2.527	<Ag5,Cu-S>		2.465	<Ag6-S>		2.537
Ag7	- S8	2.524(2)	Ag8	- S3	2.467(2)	Ag9,Cu	- S6	2.441(3)
	- S13	2.539(3)		- S13	2.485(3)		- S13	2.493(4)
	- S3	2.552(2)		- S9	2.587(2)		- S11	2.561(3)
<Ag7-S>		2.538	<Ag8-S>		2.513	<Ag9,Cu-S>		2.498
Ag10	- S12	2.505(2)	Ag11	- S14	2.511(4)	Ag12	- S14	2.446(4)
	- S13	2.512(3)		- S9	2.526(3)		- S11	2.470(3)
	- S6	2.572(2)		- S8	2.566(2)		- S12	2.549(3)
<Ag10-S>		2.530	<Ag11-S>		2.534	<Ag12-S>		2.488

$[Ag_9CuS_4]^{2+}$ B (B') layer

Cu1	- S17	2.1581(19)	Cu2	- S21	2.160(2)	Cu3	- S20	2.160(2)
	- S17	2.1581(19)		- S21	2.160(2)		- S16	2.160(2)
<Cu1-S>		2.1581	<Cu2-S>		2.160	<Cu3-S>		2.160
Ag22	- S15	2.404(3)	Ag13	- S15	2.405(2)	Ag15	- S19	2.384(2)
	- S9	2.443(3)		- S16	2.466(2)		- S7	2.419(2)
<Ag22-S>		2.424	<Ag13-S>		2.436	<Ag15-S>		2.402
Ag28	- S18	2.407(3)	Ag21	- S18	2.397(3)	Ag19	- S17	2.478(3)
	- S5	2.439(3)		- S20	2.462(2)		- S19	2.410(3)
<Ag28-S>		2.423	<Ag21-S>		2.430	<Ag19-S>		2.444
Ag23	- S19	2.431(3)	Ag18	- S18	2.448(3)	Ag27	- S15	2.450(3)
	- S21	2.461(3)		- S21	2.473(2)		- S21	2.482(3)
<Ag23-S>		2.446		- S8	2.846(3)		- S10	2.830(3)
			<Ag22-S>		2.589	<Ag22-S>		2.587
Ag30	- S22	2.530(3)	Ag25	- S22	2.513(3)	Ag29	- S22	2.564(3)
	- S17	2.547(3)		- S20	2.540(3)		- S16	2.580(3)
	- S12	2.699(3)		- S11	2.665(3)		- S6	2.614(3)
<Ag30-S>		2.592	<Ag25-S>		2.573	<Ag29-S>		2.586
Ag24	- S18	2.522(3)	Ag17	- S22	2.599(3)	Ag20	- S22	2.575(3)
	- S20	2.613(3)		- S3	2.631(3)		- S2	2.615(2)
	- S4	2.660(3)		- S16	2.715(3)		- S20	2.754(2)
<Ag24-S>		2.598		- S18	2.901(3)		- S19	2.863(3)
			<Ag17-S>		2.712	<Ag20-S>		2.702
Ag16	- S22	2.589(3)	Ag26	- S15	2.530(3)	Ag14	- S19	2.547(3)
	- S1	2.603(3)		- S17	2.583(3)		- S16	2.589(2)
	- S17	2.798(2)		- S10	2.806(3)		- S8	2.775(3)
	- S15	2.889(3)		- S11	2.934(3)		- S12	2.990(3)
<Ag16-S>		2.720	<Ag26-S>		2.713	<Ag14-S>		2.725

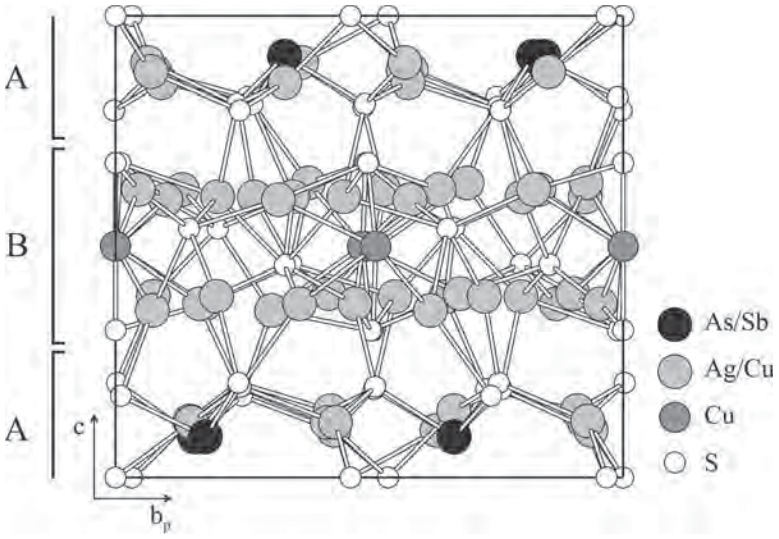

FIG. 3. Projection of the arsenpolybasite-221 structure along the *a* axis (hexagonal symmetry), emphasizing the succession of the $[(Ag,Cu)_6Sb_2S_7]^{2-}$ A (A') and $[Ag_9CuS_4]^{2+}$ B (B') module layers.

= 2.43 Å], three silver atoms (Ag7, Ag8 and Ag10) in a close to triangular coordination [$<Ag–S>_{221}$ = 2.60 Å *versus* $<Ag–S>_{222}$ = 2.59 Å], and finally a silver atom (Ag5) in approximately a tetrahedral coordination [$<Ag–S>_{221}$ = 2.71 Å *versus* $<Ag–S>_{222}$ = 2.71 Å]. The shortest cation–cation distances are: Ag–Cu: 2.794(2) Å, Ag–Ag: 3.001(2) Å, Ag–Sb: 3.4693(19) Å. The good match between the arsenpolybasite-222 and arsenpolybasite-221 structures is illustrated in Figures 4a and 4b.

DISCUSSION

The crystal structures of antimonpearceite, arsenpolybasite-221 and arsenpolybasite-222 have been solved and refined from single-crystal X-ray-diffraction data. As already observed for polybasite-222 (Evain *et al*. 2006a), the complexity of the determination of the arsenpolybasite-222 structure comes from the apparent trigonal symmetry linked to a second-degree twinning by metric merohedry of the real monoclinic structure. It should be stressed that in both the arsenpolybasite-222 and polybasite-222 structures, all the atom positions, except those of the Ag atoms in the $[Ag_9CuS_4]^{2+}$ B pseudo layer, approximately follow a mirror (*m*[010]) symmetry operation. Therefore, through the combination with the *c* glide-mirror symmetry operation of the *C*2/*c* space group, they are approximately translated by ½ along the *c* axis. This feature, along with the absence of the *h*0*l*, $l = 2n + 1$ systematic extinction because of the twinning, could explain why *C*2/*m* was mistakenly considered to be the correct space-group and why the structure could not be solved until now.

The 222 structures show the –AB–A'B'–AB–A'B'– double-layer module sequence (present study, Evain *et al*. 2006a); thus they can be considered as polytypes of the 221 structures with sequence –AB–AB– (present study, Evain *et al*. 2006a), the A'B' double-layer module being related to AB by a glide reflection perpendicular to the *b* axis with translational component **c**/2. However, the AB_{221} module is not strictly equivalent in chemical composition to the AB_{222} (or $A'B'_{222}$) module, the 221 structures being richer in copper (present study, Evain *et al*. 2006a). It seems that the higher the Cu content, the more likely is the structure to be of the 221 type. As is generally the case, the higher the disorder, the higher the apparent symmetry. With a limited substitution of Cu for Ag, the crystal system is monoclinic with a double *c* period (*i.e.,* 222 structures). However, the AB (A'B') double-layer module has a pseudotrigonal symmetry, which explains the twinning and the apparent hexagonal cell. By increasing the extent of the substitution of Cu for Ag, the cell doubling along the *c* direction is lost, and the average symmetry becomes trigonal (*i.e.,* 221 structures). A further increase of the disorder gives rise to a folding of the cell along the *a* and *b* directions, as found in the 111 structures (present study, Bindi *et al*. 2006a). Our findings support the idea of Hall (1967), who suggested that the variation of Cu content in different samples might be the driving force of different unit-cell stabilizations.

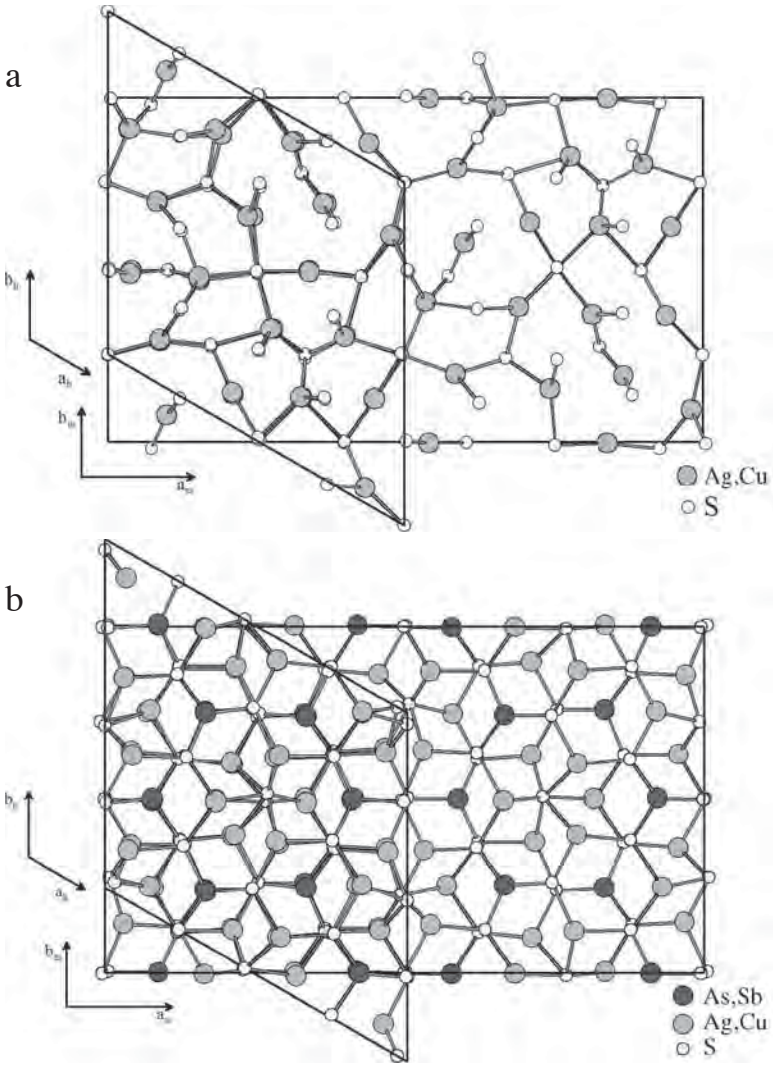

FIG. 4. Superposition, down the *c* axis, of equivalent fractions of the $[(Ag,Cu)_6(As,Sb)_2S_7]^{2-}$ A (a) and $[Ag_9CuS_4]^{2+}$ B (b) module layers of arsenpolybasite-222 and arsenpolybasite-221, showing the good match between the two structures.

In summary, we found that the minerals of the pearceite–polybasite group exhibit three types of unit cell (*i.e.*, 111, 222, and 221) that correspond to three separate structures (space group $P\bar{3}m1$, $P321$, and $C2/c$ for 111, 221, and 222, respectively). The determination of the crystal structures of all the members of the group allows to consider them as a family of polytypes, since they are built up of layers of nearly identical structure and composition stacked along the **c** axis. For this reason, a proposal to change the existing nomenclature has been submitted to the IMA–CNMNC.

ACKNOWLEDGEMENTS

The authors are grateful to Prof. Paul G. Spry (Iowa State University, Ames, Iowa) for his help with the electron-microprobe analyses. The paper benefitted from the official reviews made by Andrew Locock and an anonymous reviewer. The authors are also grateful to Robert F. Martin for his suggestions on improving the manuscript. This work was funded by C.N.R. (Istituto di Geoscienze e Georisorse, sezione di Firenze) and by M.I.U.R., P.R.I.N. 2005 project "Complexity in minerals: modulation, modularity, structural disorder".

References

Bachmann, R. & Schulz, H. (1984): Anharmonic potentials and pseudo potentials in ordered and disordered crystals. *Acta Crystallogr.* **A40**, 668-675.

Becker, P. J. & Coppens, P. (1974): Extinction within the limit of validity of the Darwin transfer equations. I. General formalism for primary and secondary extinction and their applications to spherical crystals. *Acta Crystallogr.* **A30**, 129-147.

Bindi, L., Evain, M. & Menchetti, S. (2006a): Temperature dependence of the silver distribution in the crystal structure of natural pearceite, $(Ag,Cu)_{16}(As,Sb)_2S_{11}$. *Acta Crystallogr.* **B62**, 212-219.

Bindi, L., Evain, M., Pradel, A., Albert, S., Ribes, M. & Menchetti, S. (2006b): Fast ionic conduction character and ionic phase-transitions in disordered crystals: the complex case of the minerals of the pearceite–polybasite group. *Phys. Chem. Minerals* **33**, 677-690.

Boucher, F., Evain, M. & Brec, R. (1993): Distribution and ionic diffusion path of silver in γ-Ag_8GeTe_6: a temperature dependent anharmonic single crystal structure study. *J. Solid State Chem.* **107**, 332-346.

Brandenburg, K. (2001): *Diamond version 3*. Crystal Impact GbR, Bonn, Germany.

Edenharter, A., Koto, K. & Nowacki, W. (1971): Über Pearceit, Polybasit und Binnit. *Neues Jahrb. Mineral., Monatsh.*, 337-341.

Engel, P. & Nowacki, W. (1966): Die Verfeinerung der Kristallstruktur von Proustit, Ag_3AsS_3, und Pyrargyrit, Ag_3SbS_3. *Neues Jahrb. Mineral.. Monatsh.*, 181-184.

Evain, M., Bindi, L. & Menchetti, S. (2006a): Structural complexity in minerals: twinning, polytypism and disorder in the crystal structure of polybasite, $(Ag,Cu)_{16}(Sb,As)_2S_{11}$. *Acta Crystallogr.* **B62**, 447-456.

Evain, M., Bindi, L. & Menchetti, S. (2006b): Structure and phase transition in the Se-rich variety of antimonpearceite, $[(Ag,Cu)_6(Sb,As)_2(S,Se)_7][Ag_9Cu(S,Se)_2Se_2]$. *Acta Crystallogr.* **B62**, 768-774.

Evain, M., Gaudin, E., Boucher, F., Petříček, V. & Taulelle, F. (1998): Structures and phase transitions of the A_7PSe_6 (A = Ag,Cu) argyrodite-type ionic conductors. I. Ag_7PSe_6. *Acta Crystallogr.* **B54**, 376-383.

Frondel, C. (1963): Isodimorphism of the polybasite and pearceite series. *Am. Mineral.* **48**, 565-572.

Gaudin, E., Boucher, F. & Evain, M. (2001): Some factors governing Ag^+ and Cu^+ low coordination in chalcogenide environments. *J. Solid State Chem.* **160**, 212-221.

Hall, H.T. (1967): The pearceite and polybasite series. *Am. Mineral.* **52**, 1311-1321.

Harris, D.C., Nuffield, E.W. & Frohberg, M.H. (1965): Studies of mineral sulphosalts. XIX. Selenian polybasite. *Can. Mineral.* **8**, 172-184.

Herrendorf, W. (1993): *Habitus*. PhD dissertation, University of Karlsruhe, Germany.

Johnson, C.K. & Levy, H.A. (1974): International Tables for X-ray Crystallography IV (J.A. Ibers & W.C. Hamilton, eds.). Kynoch Press, Birmingham, U.K. (311-336).

Kuhs, W.F. (1984): Site-symmetry restrictions on thermal-motion-tensor coefficients up to rank 8. *Acta Crystallogr.* **A40**, 133-137.

Kuhs, W.F. (1992): Generalized atomic displacements in crystallographic structure analysis. *Acta Crystallogr.* **A48**, 80-98.

Kuhs, W.F. & Heger, G. (1979): Neutron diffraction study of copper sulfide bromide (Cu_6PS_5Br) at 293 K and 473 K. In Fast Ion Transport in Solids: Electrodes and Electrolytes. (P. Vashishta, J.N. Mundy & G.K. Shenoy, eds.). Elsevier, Amsterdam, The Netherlands (233-236).

Minčeva-Stefanova, I., Bonev, I. & Punev, L. (1979): Pearceite with an intermediate unit cell – first discovery in nature. *Geokhim. Mineral. i Petrol.* **11**, 13-34 (in Bulg.).

Nespolo, M. (2004): Twin point groups and the polychromatic symmetry of twins. *Z. Kristallogr.* **219**, 57-71.

Peacock, M.A. & Berry, L.G. (1947): Studies of mineral sulphosalts. XIII. Polybasite and pearceite. *Mineral. Mag.* **28**, 1-13.

Petříček, V., Dušek, M. & Palatinus, L. (2000): *JANA2000, a Crystallographic Computing System*. Institute of Physics, Academy of Sciences of the Czech Republic, Prague, Czech Republic.

Pfitzner, A., Evain, M. & Petříček, V. (1997): $Cu_{12}Sb_4S_{13}$: a temperature-dependent structure investigation. *Acta Crystallogr.* **B53**, 337-345.

Ribár, B. & Nowacki, W. (1970): Die Kristallstruktur von Stephanit, $[SbS_3|S|Ag_5^{III}]$. *Acta Crystallogr.* **B26**, 201-207.

Savelsberg, G. & Schäfer, H. (1978): Preparation and crystal structure of sodium silver arsenide (Na_2AgAs) and potassium copper sulfide (KCuS). *Z. Naturforsch.* **33b**, 711-713.

Shannon, R.D. (1981): Bond distances in sulfides and a preliminary table of sulfide crystal radii. *In* Structure and Bonding in Crystals II (M. O'Keeffe & A. Navrotsky, eds.). Academic Press, New York, N.Y. (53-70).

Stoe & Cie (1996): *X-shape (version 1.02)*. Stoe & Cie, Darmstadt, Germany.

Sugaki, A., Kitakaze, A. & Yoshimoto, T. (1983): Synthesized minerals of polybasite and pearceite series – synthetic sulfide minerals (XII). *Sci. Rep. Tohoku Univ., Ser. 3: Mineralogy, Petrology and Economic Geology* **15**, 461-469.

Received April 9, 2006, revised manuscript accepted September 17, 2006.